

Deposition of Cohesive Sediments under Waves  
S. Abdel-Mawla      A. Matheja      C. Zimmermann

*Abstract*

The deposition of cohesive sediment depends on a combination of different factors, including size, settling velocity and strength of the settling units. It may be hypothesised, that deposition of flocs is controlled by stochastic turbulent processes in a zone near the bed. A large difference exists in the basic characteristics of the response of water-mud system to wave-induced motion. In this paper, a physical model is studied for deposition of natural cohesive sediments under regular waves. Measuring velocities and dynamic pressure on the bottom, the bottom shear stress can be estimated. It is found, that at very close values of bottom shear stress, the rate of deposition is changed according to the pressure steepness on the bottom.

*Introduction*

Siltation of harbours and coastal zones is often undesirable as it diminishes navigability. Besides, deposited mud is often polluted, because it specifically absorbs contaminants from water. For managers of harbours and coastal zones it is therefore important to know prior to execution whether planned projects will diminish or increase siltation. The performance of the current cohesive sediment transport models, which are being used as a tool for making prediction, is sometimes disappointing and therefore needs further improvement. The shortcomings are caused to a great extent by an insufficient knowledge of mechanisms underlying cohesive sediment transport.

Cohesive sediment mainly consisting of clay particles, which may be single or more likely aggregation of flocs. The deposition mechanism of these particles can be concluded in fig. 1. For more comprehensive discussion the reader is referred to Mehta et al. (1989), Mehta (1993, 1996) and Pathirana and Berlamont (1994).

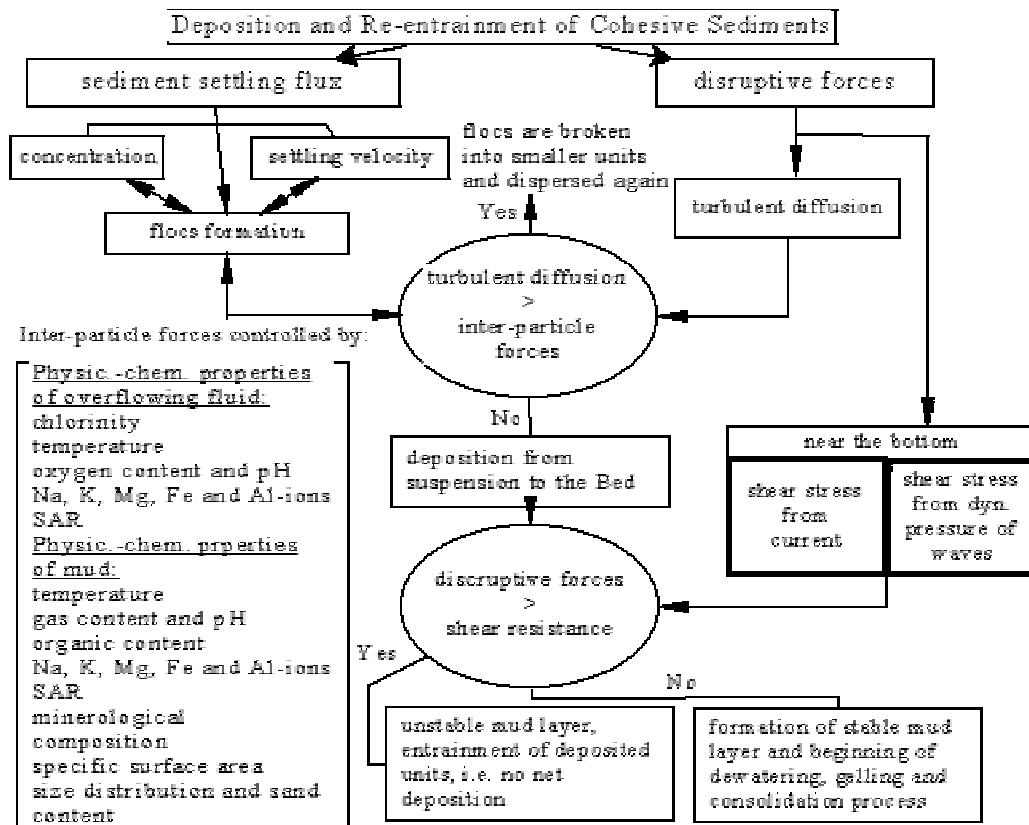


Fig. 1. Deposition Mechanism of Cohesive Sediments

### Literature Review

In most of cohesive sediment deposition models, as presented by Teisson et al. (1993) or Mehta (1996), deposition was modelled according to Krone (1962):

$$dm / dt = (1 - \tau_b / \tau_d) w_s c \quad (1)$$

This empirical formula is developed for current. It is used also to model the process for waves as the deposition process is qualitatively similar. Settling velocity is described by Mehta (1984), who discussed the role of physico-chemical properties in modifying the sediment characteristics and produced the following empirical equations:

$$w_s = k_1 c^n \quad \text{for } c = 0.3 \text{ to } 3.5 \text{ g/l} \quad (2)$$

$$w_s = w_{s0} (1 - k_2 c)^\beta \quad \text{for } c = 3.0 \text{ to } 15.0 \text{ g/l} \quad (3)$$

Hawang (1989) developed a formula for settling velocity in flocculation and hindered settling regions:

$$w_s = \frac{a c^n}{(c^2 + b^2)^m} \quad (4)$$

Mimura (1993) studied the rates of erosion and deposition of cohesive sediments under wave action. Bottom shear stress is calculated using the wave friction factor (Jonsson, 1966). The author found, that deposition and erosion coexist in some range of bottom shear stress.

De Wit (1994, 1995) studied the effect of pore water pressure change in the mud layer on the liquefaction process. The author found the mud liquefying when pressure-induced shear stresses in the bed exceed the yield strength of the mud. Some of previous experimental studies in the field of cohesive sediments is concluded in tab. 1. In this study, an attempt was made to estimate the bottom-shear stress using the measured velocity components to define the role of dynamic wave pressure on the deposition procedure.

Table 1. Laboratory Facilities for Prior Studies

\* t=bed sample thickness \*\* d=water depth over the bed \*\*\*T,H =wave period and height

Authors / Objective	Nature of Soil Samples	Lab. Facility	Flow Condition
Otsubo (1988) erosion	artificial kaolinite, bentonite, natural mud (t = 2 cm)	pipe with fresh water (d = 5 cm)	steady currents
Parchure and Mehta (1985) erosion	commerical kaolinite mixed with tap water and salt	rotating annular flume (d = 26cm)	uniform turb. shear flow current
Yamamoto(1984) erosion	bentonite clay mixed with sea water (t = 69 cm)	wave flume (d = 40 cm)	reg. waves, diff. T and H
Horikawa (1986) erosion	artificial kaolinite mixed with water (diff. $w_c$ ), (t = 9.5 cm)	wave flume (d = 10 cm)	reg. waves, T = 1 s, H = 1.5-1.7 cm
de Wit (1995) erosion	artificial china and westwald clay (t = 20 cm)	wave flume	reg. waves, current, T = 1.5s, H = 1.5-9.3 cm
Feng (1992) bed fluidization	kaolinite clay (t = 16 cm)	wave flume (d = 35 cm)	reg. waves, T = 1.0 s, diff. H
Li (1996) entrainment	natural cohesive sed. (t = 15 cm)	wave flume (d = 60 cm)	reg. waves, T = 0.8-1.6 s, H = 1-8cm
van Kessel (1997) erosion and liquefaction	china clay, natural mud (t = 10 cm)	wave flume (d = 30 cm)	reg. waves, T = 1.65s, H = 0.4-5.5 cm

#### Experimental set-up and procedure

The wave flume shown in fig. 2 has been used. The water depth is kept constant at 40 cm. The bed is kept fixed. Near the middle of the flume the instruments are mounted to measure the local developments of the deposition process. Acoustic doppler velocimeter (ADV), spectrophotometer (SPM), pressure transducer (PM) and two wave height meters (WHM) were used to measure velocity components, sediments concentration, pressure fluctuation on the bed and wave height respectively.

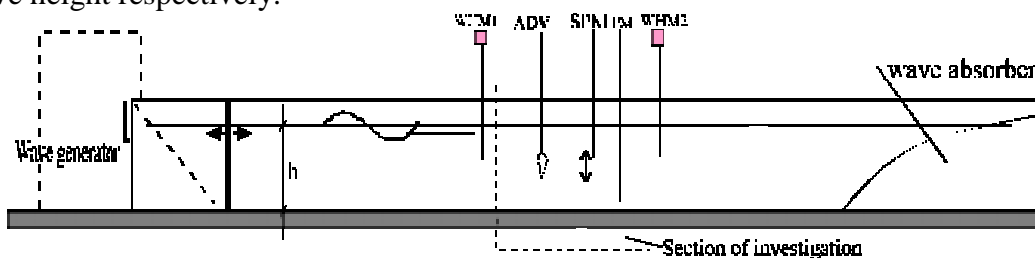


Fig. 2. Sketch of the Wave Flume

Experiments cover a range of wave characteristics (wave periods of 0.74, 0.87, 1.06, 1.40 s and wave heights from 0.88 cm to 10.5 cm) and three initial concentration ratios (3.5, 8.0 and 12.0 g/l). The suspensions with 8.0 and 12.0 g/l were tested for wave periods of 0.74 s and 1.40 s.

The cohesive material is a natural clay imported from an under ground clayey strata (tab. 2 to tab. 6). According to Mehta and Jiang (1996), the settling velocity formula of Hawang (1989) from (4) was calibrated by an experiment using settling column ( $a = 0.14$ ,  $b = 49$ ,  $n = 1.3$  and  $m = 2.3$ ). The mixing trough all the flume ends, when samples give the required initial concentration  $c_0$ . A small volume configuration (3mm) of ADV is used to measure velocity fluctuations near to the bottom and along the water column.

For each measuring point, more than 50 waves were measured. The sampling frequency of ADV (0.1 to 25 Hz) is adjusted according to the used wave period.

#### Data Analysis

Turbulent and wave-induced components of the free surface elevations and velocities were separated by phase averaging over 50 waves. Using this technique the local wave height and the setdown and setup were evaluated. Phase-averaged horizontal velocities are used to estimate the shear velocity. Wave-induced current  $\bar{u}_a$  is included in the phase-averaged  $u_a$  since it would be difficult to analyze the oscillatory component  $u_a - \bar{u}_a$  and the mean component  $u_a$  separately (nonlinearity of the bottom shear stress). Near the bottom, a logarithmic velocity profile is assumed at each phase over the wave period:

$$u_a(Z_b) = \frac{u_*}{\kappa} \ln(Z_b - d_* / Z_0) \quad \text{for } Z_b \geq (d_* + Z_0) \quad (5)$$

Jackson (1981) showed, that the expression of  $d_* = 0.7$  times the roughness height was a adequate estimate in many commonly encountered types of roughness. After Cox et al. (1996) (5) can be reduced to a linear equation:

$$Y_i = \beta X_i + \alpha \quad \text{for } i = 1, 2, \dots, n \quad (6)$$

$$X_i = [u_a]_i \quad \text{and} \quad Y_i = \ln[(Z_b)_i - d_*] \quad (7)$$

$$\beta = \kappa / u_* \quad \text{and} \quad \alpha = \ln(Z_0) \quad (8)$$

Maximum shear velocity  $U_*$  and bottom roughness  $Z_0$  for specified  $\kappa = 0.4$  and  $d_* \cong 0.7 d_{50}$  ( $d_{50} = 0.90$  mm) were computed using the least squares procedure. The actual value of  $d_*$  is selected as the best fit among  $d_* = 0.04$ ,  $0.05$ ,  $0.07$  and  $0.08$ , because the elevation  $Z_b$  includes the uncertainty of the initial elevation of the ADV measuring volume. Values for  $U_*$  and  $Z_0$  are computed three times for  $n = 3$ ,  $4$  and  $5$ . The best fit is selected by the square of the correlation coefficient  $\gamma_{xy}^2$ .

Following Jonsson and Carlsen (1976) temporal variation of bottom shear stress for sinusoidal flow is given by:

$$\tau_b(t) = \rho |u_*| u_* \quad \text{with } u = \sqrt{(f_w / 2)} U_b \cos(\omega t) \quad (9)$$

The friction factor  $f_w$  is assumed to be constant over the wave cycle and is determined from the peak values at  $t = 0$ :

$$f_w = \frac{2U_*^2}{U_b^2} \quad (10)$$

The near-bottom maximum horizontal velocity  $U_b$  based on linear wave theory is given in (11). The variation of bottom shear stress is expressed after van Rijn (1993) in (12). Neglecting the phase shift between bottom shear stress and velocity immediately outside the boundary layer and assuming the maximum bottom shear stress affect within a short part of the wave period, the use of time-averaged bed shear stress (over half a wave cycle) is more realistic as shown in (13). The rate of deposition  $R_d$  is calculated from the concentration profiles with (14).

$$U_b = \frac{H\omega}{2\sinh(kh)} \quad (11)$$

$$\tau_b(t) = \frac{1}{2} \rho f_w U_b^2 \quad (12)$$

$$\tau_b = \frac{1}{4} \rho f_w U_b^2 \quad (13)$$

$$R_d = \frac{1}{t} \int_{t=i}^{t=i+1} \int_{z=0}^{z=h} C(z,t) dz dt \quad (14)$$

### Results

Experiments running time increased according to the used wave characteristics or in other words, when the water column sediments settle down very slowly. The running time reached up to 24 hours. Measuring the concentration profiles each time and according to equation (16), the time-total deposited sediments relationships are drawn for all wave characteristics and initial sediment concentrations used in this study. Deposition under still water ( $H/gT^2=0$ ) was taken as a reference for the deposition behaviour.

It is found that data has a good logarithmic fitting. This can be explained by sorting and flocculation mechanism of cohesive sediments, which occur during deposition. Fig. 3 is an examples for this group of relationships. As shown, the rate of deposition decreases as the wave height increase at the same wave period. Comparing fig. 3 (a) and (b), it is found that the rate of deposition for  $c_0 = 8.0$  g/l is more than for 4.0 g/l. This can be explained by increasing settling velocities due to increasing concentration up to a certain limit (flocculation limit from (5) is about 12 g/l). Fig. 4 conclude all used wave conditions, expressed as dimensionless parameters ( $H/gT^2$  and  $h/gT^2$ ), against deposited sediments for initial concentration 3.5 g/l. Comparing the behaviour of deposition it is found that as  $(h/gT^2)$  increases, the effect of wave steepness ( $H/gT^2$ ) decreases and deposition increases at the same wave steepness.

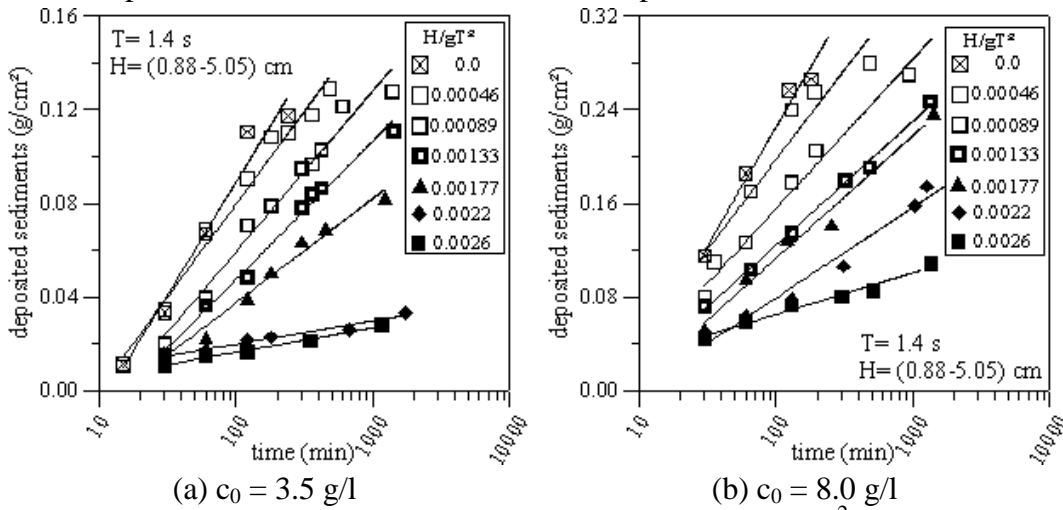


Fig. 3. Time-total Deposited Sediment Relation for  $h/gT^2 = 0.021$

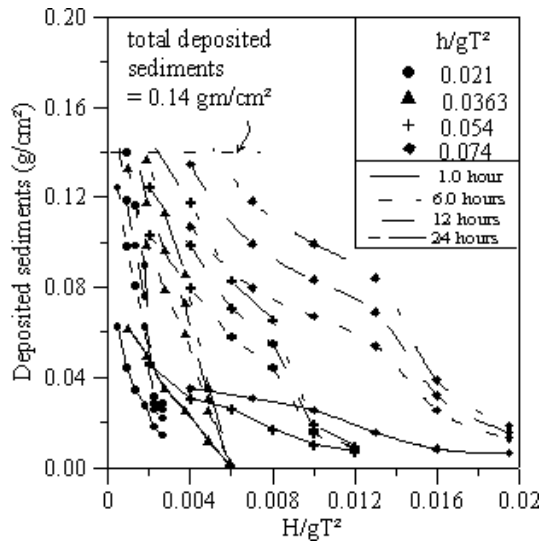


Fig. 4. Development of Total Deposited Sediment with Time under different Wave Conditions

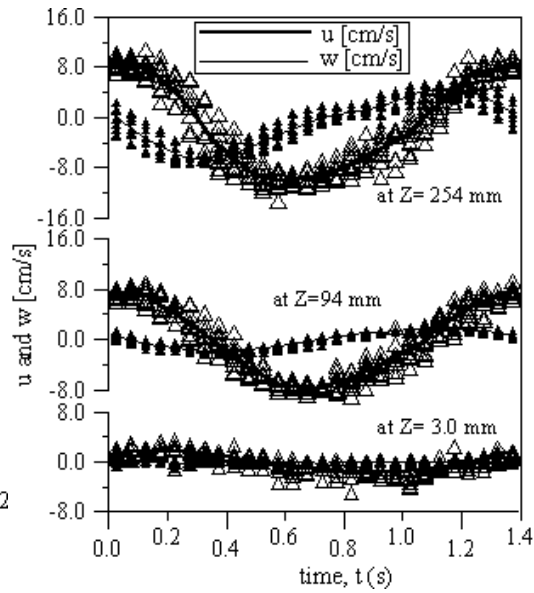


Fig. 5. Calculated Phase-averaged Velocities for Measured Data ( $h/gT^2 = 0.021$  and  $H/gT^2 = 0.00263$ )

The phase averaged velocities are calculated at each measuring points. Fig. 5 shows an example including data scattering. Fig. 6 shows an example for the results of application the algorithm explained through (6) to (9).

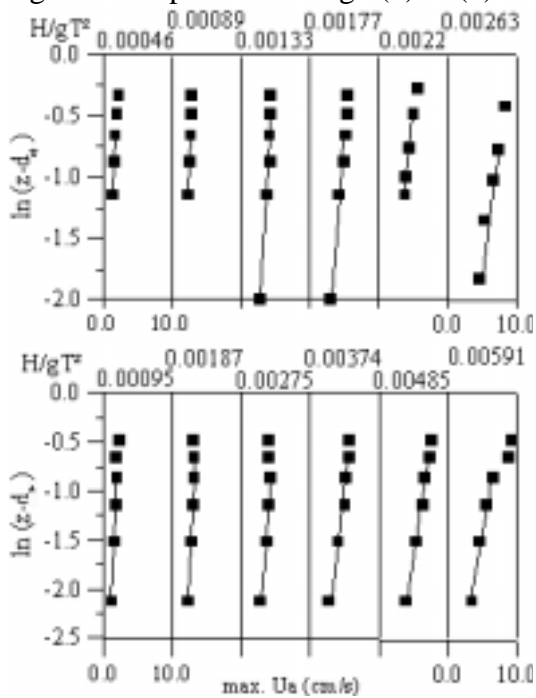


Fig. 6. Central Variations of Max. Phase-averaged Horizontal Velocity  $U_a$

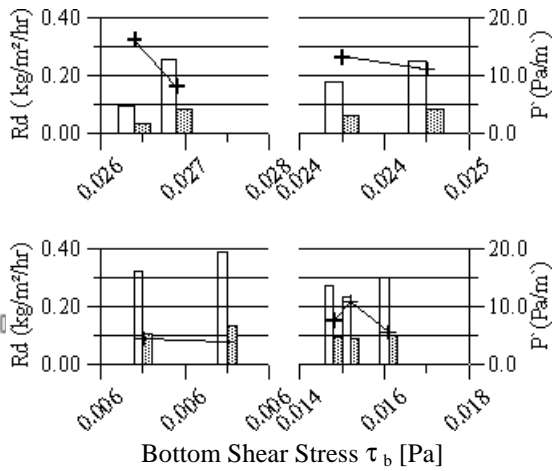


Fig. 7. Rate of Deposition for Nearly Identical Shear Stress Values ( $c_0 = 3.5$  g/l)

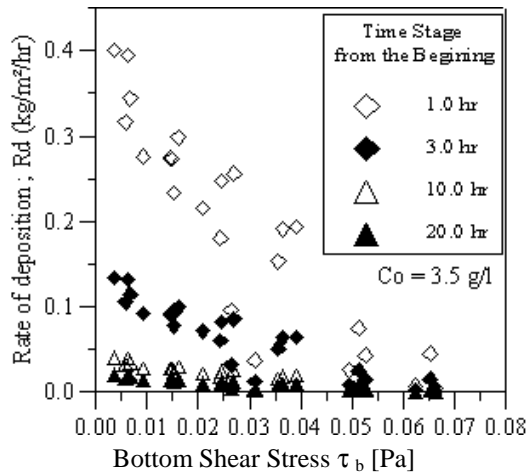


Fig. 8. Effect of Bottom Shear Stress on the Rate of Deposition

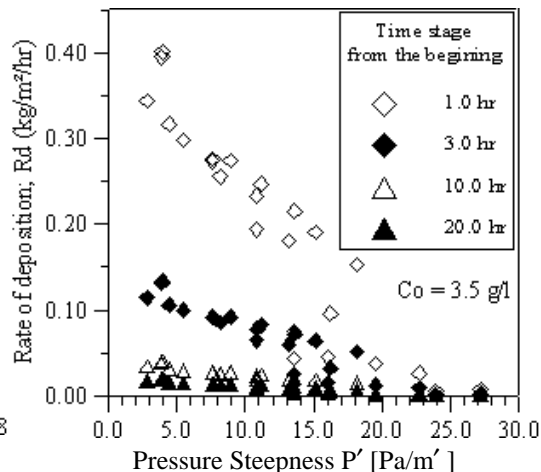


Fig. 9. Effect of Pressure Steepness on the Rate of Deposition

The estimated bottom shear stress in (13) is studied against the rate of deposition at different time steps (fig. 7 for  $c_0 = 3.5$  g/l). Measured dynamic wave pressure on the bottom is studied also against the rate of deposition. It is found that the relation has a more understandable trend, when pressure is expressed as a steepness ( $P/gT^2$ ). As shown in figs. 8 and 9, the rate of deposition is decreased as bottom shear stress and pressure steepness increase.

Looking through all the bottom shear stress values and selecting some very close values, the rate of deposition is studied against these nearly identical shear stress values (fig. 7). It is notable, that rate of deposition decrease as the pressure steepness increases.

#### Conclusion

Flocculation and sorting processes always control deposition of cohesive sediments, which can be notified in all test cases.

The sediment deposition decreases as ( $h/gT^2$ ) decreases for same wave steepness values, because bottom shear stress and diffusion coefficient under these conditions increase.

It is found, that not only the bottom shear stress controls the deposition of cohesive sediments, but also the pressure steepness has this role. The probability factor stated in (1) should incorporate the pressure steepness also to express the deposition mechanism under waves more properly. This will be done by studying wide ranges of initial concentrations, water depths and wave characteristics, which is under research at the moment.

#### Appendix I. References

- Cox, D.T., Kobayashi, N., and Okayasu, A. (1996). "Bottom shear stress in surf zone." *J. Geophys. Res.*, 101(c6 14), 337-348.
- De Wit, P.J. (1995). "Liquefaction of cohesive sediments caused by waves." Rep. No. 95-2, Ph. D. thesis, Delft University of Technology, Delft, Netherlands.
- De Wit, P.J. (1994). "Liquefaction and erosion of mud due to waves and current - Experiments on China Clay." Rep. No. 10-92, Delft University of Technology, Delft, Netherlands.
- Feng, J. (1992). "Laboratory experiments on cohesive soil bed fluidization by water waves." M.S. thesis, University of Florida, Gainesville, Florida.
- Hawang, K. (1989). "Erodibility of fine sediment in wave-dominated environments." M.S. thesis, University of Florida, Gainesville, Florida.
- Horikawa, K. and Shibayma T. (1986). "Mud mass transport due to waves." *Coastal Engineering in Japan*, Vol. 29, 151-161.
- Jonsson, I. G. (1966). "Wave boundary layers and friction factors." In: *Proc. of the 10th Coastal Eng. Conf.*, 127-148, ASCE, New York.
- Jackson, P.S. (1981). "On the displacement height in the logarithmic velocity profile." *J. Fluid Mech.*, Vol. 111, 15-25.
- Jonsson, I.G., and Carlsen, N.A. (1976). "Experimental and theoretical investigations in an

oscillatory turbulent boundary layer." *J. Hydraul. Res.*, Vol. 14, 45-60.

Krone, R.B. (1962). "Flume studies of the transport of sediments in estuarial shoaling processes." Final Rep., Hydraulic Engineering Laboratory and Sanitary Engineering Research Laboratory, University of California, Berkeley.

Li, Y. (1996). "Sediment-associated constituent release at the mud-water interface due to monochromatic waves." Ph. D. thesis, University of Florida, Gainesville, Florida.

Mehta, A. (1984). "Characterization of cohesive sediment properties and transport processes in estuaries." In: *Estuarine Cohesive Sediment Dynamics*, Mehta, A.J. (Ed.), Lecture notes on coastal and estuarine studies, Vol. 14, 290-315.

Mehta, A., McAnally, W., Hayter, J., Teeter, A., Heltzel, S. and Carey W. (1989). "Cohesive sediment transport. II: Application." *J. Hydr. Eng.*, 115 (8), ASCE, 1094-1112.

Mehta, A.J. and Jiang, F. (1993). "Some observations on bottom mud motion due to waves." Report UFL/coel/mp-93/01, Coastal and Oceanographic Eng. Dept., University of Florida, Gainesville, Florida.

Mehta, A. (1996). "Interaction between fluid mud and water waves." *Env. Hydr.*, Kluwer Academic Publishers, 153-187.

Mimura, N. (1993). "Rates of erosion and deposition of cohesive sediments under wave action." In: *Near shore and estuarine cohesive sediment transport*, Mehta, A.J. (Ed.), 247-264.

Otsubo, K. and Muraoka, K. (1988). "Critical shear stress of cohesive bottom sediments." *J. Hydr. Eng.*, 114 (10), 1214-1256.

Pathirana, C. and Berlamont, J (1994). "Modelling Cohesive Sediment Transport in Tidal Waters." *Int. Conf. Port and Harbor Construction*, Vol.2, Yokosuka, Japan, 1271-1290.

Parchure, M. and Mehta, A. (1985). "Erosion of soft cohesive sediment deposits." *J. Hydr. Eng.*, 111 (10), ASCE, 1308-1326.

Teisson, C., Ockenden, M., Kranburg, C. and Hamm, L. (1993). "Cohesive sediment transport processes." *Coast. Eng.*, Vol. 21, 129-162.

van Rijn, L.C. (1993). "Principles of sediment transport in rivers, estuaries and coastal seas." Aqua Publications, Netherlands.

van Kessel, T. (1997). "Generation and transport of subaqueous fluid mud layers." Rep. No. 97-5, Dept. Civ. Eng., Delft University of Technology, Delft, Netherlands.

Yamamoto, T. (1984). "A laboratory experimentation on the interactions between water waves and soft clay beds." *Coast. Eng. in Japan*, Vol.27, 279-291.

#### *Appendix II. Notation*

The following symbols are used in this paper:

$\tau_b$	=	bottom shear stress []
$\tau_d$	=	critical shear stress for deposition []
$w_s$	=	settling velocity [m/s]
$k_1, k_2$	=	empirical coefficients depending on sediment composition
$n$	=	coefficient vary between 1 and 2
$w_{so}$	=	reference settling velocity, found to be 5.0
$c$	=	concentration [kg/m <sup>3</sup> ]
$a, b, n, m$	=	sediment dependent empirical coefficients
		$b=1$ to 10, $n=0.8$ to 2.5, $m=1$ to 3
$u_a$	=	phase-averaged horizontal velocity []
$Z_b$	=	vertical coordinate (upward) with $Z_b = 0$ at the bottom of the flume []
$u_*$	=	shear velocity []
$k$	=	van Karman constant 0.4
$d_s$	=	displacement distance



$Z_0$	=	bottom roughness
$\rho$	=	fluid density
$f_w$	=	wave friction factor
$U_b$	=	maximum horizontal velocity near the bottom
$\omega$	=	angular frequency
$H$	=	local wave height
$\bar{h}$	=	local mean water depth, including wave set-up/set-down
$\bar{h} = d + \overline{\eta_a}$	=	phase-averaged free surface elevation
$k$	=	local wave number

*Subscripts*

$i$	=	measuring point elevation, such that $(Z_b)_i = 0.2, 0.3, 0.4, 0.5$ and $0.6$ for $i = 1, 2, 3, 4$ and $5$
$n$	=	number of points used for the logarithmic fit $n = 3, 4$ and $5$